Salinity Stratification from a Navigation Canal into a Shallow Lake

Ioannis Y. Georgiou, Alex J. McCorquodale
Department of Civil Engineering, University of New Orleans, New Orleans, Louisiana, 70148
igeorgiou@uno.edu, jmccorqu@uno.edu

Abstract

This paper demonstrates the behavior of a dense plume originating in a navigation canal and intruding into a shallow lake. The navigation canal, being connected to Gulf of Mexico brings saline water (>20 ppt) into the brackish lake (~6 ppt). This higher density plume descends and spreads radially in a thin layer at the bottom of the lake. The plumes' interface sustains high density gradients often resulting in low oxygen transfer to the bottom waters near the lake bed. The density gradients are relatively stable and vertical mixing is at minimum under fair wind shear. Plume stability analysis indicates that wind shear induced by wind speeds of 11 m/s and a fetch of 30 Km can produce plume instability, therefore promote vertical mixing throughout the water column. Wind observations in the area have shown that required winds for destratification of the plume are primarily during winter months.

Introduction

The Inner Harbor Navigational Canal (IHNC) is part of the Mississippi River Gulf Outlet (MRGO), which permits ships to navigate from the Gulf of Mexico to Lake Pontchartrain and the Mississippi River at New Orleans (Figure 1). The IHNC is a deep channel with a mean depth near its connection to the Lake of about 10 m. Lake Pontchartrain is a relatively shallow, brackish estuarine lake with a mean depth of less than 4 m and a mean salinity of 4 ppt. At times, the IHNC brings highly saline water (>20 ppt) into Lake Pontchartrain. Under certain conditions, this higher density water has been observed to form a layer of high salinity water over a large area of the bottom of the Lake (300 km^2). This layer is often associated with low dissolved oxygen (DO) and at times becomes hypoxic, a condition that is harmful to shellfish. The salinity wedge in the IHNC had a depth that was typically greater than 60 – 80 % of the canal depth (10 m) while outside of the canal entrance the depth of the density layer was of the order of 0.5 m compared to the mean lake depth of 4 m. The elevation of the saltwater wedge in the canal is typically 2 – 3 m higher than the lake bottom. This difference in the density plume elevation causes a saltwater flux into Lake Pontchartrain.

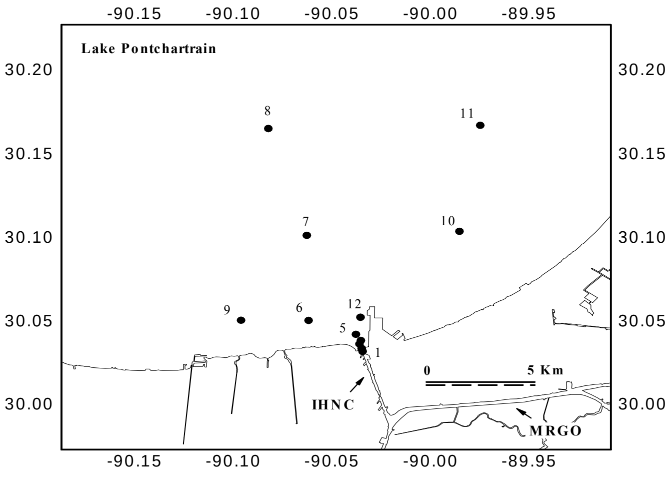

Figure 1 Aerial view of the plume area showing the points for the field sampling program

The summer observations usually showed hypoxia within the stratified layer, but no hypoxia outside of this layer. Data during winter showed high salinity stratification, but no hypoxia. It is thought that the dominant winds out of the north, north-west, and north-east in the winter cause greater vertical mixing and more frequent destabilization of the plume thus resulting in an increase in the bottom DO. The low winter water temperatures also result in higher saturation values for the DO and a reduced bacterial demand for DO. In the summer there are more southerly winds which have a short fetch with respect to the plume location and therefore result in smaller waves and less vertical mixing. The Princeton Ocean Model (POM) is being applied to study the dynamic behavior of the saltwater plume. Forcing functions for the POM model include tide and wind effects. In the future, this model will be applied to study the effect of Lake currents on the location and stability of the plume. In addition, a physical model has been constructed and operated to assess the spreading behavior of the density wedge and the effect of introducing a sill to control the saltwater flux into Lake Pontchartrain.

Background

The stability of a saltwater-freshwater interface, among other things, is related to the gradient Richardson number through the expression shown in Eq. 1 (Yih, 1980).

$$Ri = \frac{g}{\rho}\frac{\left(\frac{\partial \rho}{\partial y}\right)}{\left(\frac{\partial u}{\partial y}\right)^{2}} \qquad [1]$$

where Ri = gradient Richardson number, ρ = density of fluid, y = water depth, u = total velocity component near the bed (includes u_{cur} = near-bed current velocity, u_s = wave orbidal velocity), and g = acceleration of gravity. In general, mixing is inhibited at and below the interface of the saltwater lens. At high values of the Richardson number, there is no mass exchange taking place across the shear interface, but there is exchange of momentum even if the shear produces perturbations without breaking (Kjerfve, 1988). High velocities induced by wind shear, associated wave action, and near-bed current velocities can destabilize the interface. In shallow water, wind speed, fetch, and depth greatly affect the development of waves (Laenen and Tourneau, 1996). Using wave forecasting equations used by the U.S. Army Corps of Engineers (1984) along with orbital velocities based on linear wave theory, and by obtaining information on near-bed current velocities from numerical models (Haralampides, 2000), values for the total near-bed velocities were obtained by superposition. Eqs. 2, 3, 4 and 5 were used to calculate the wave height (H_s), wave length in shallow water (L_s), and the wave period (T_s).

$$T_s = 7.54\left(\frac{U_A}{g}\right)\tanh\left(0.833\left(\frac{gh}{U_A^{2}}\right)^{0.375}\right)\tanh\left(\frac{0.0379\left(\frac{gF}{U_A^{2}}\right)^{0.333}}{\tanh\left(0.833\left(\frac{gh}{U_A^{2}}\right)^{2}\right)}\right) \qquad [2]$$

$$L_s = \left(\frac{gT^{2}}{2\pi}\right)\tanh\left(\frac{2\pi h}{\left(\frac{gT^{2}}{2\pi}\right)}\right) \qquad [3]$$

$$H_s = 0.283\left(\frac{U_A^{2}}{g}\right)\tanh\left(0.530\left(\frac{gh}{U_A^{2}}\right)^{0.75}\right)\tanh\left(\frac{0.00565\left(\frac{gF}{U_A^{2}}\right)^{0.5}}{\tanh\left(0.530\left(\frac{gh}{U_A^{2}}\right)^{0.75}\right)}\right) \qquad [4]$$

$$u_s = \frac{\pi H}{T_s \sinh\left(\frac{2\pi h}{L_s}\right)} \qquad [5]$$

where T_s is the significant wave period, U_A is the effective wind speed, g is the acceleration of gravity, F is the effective fetch, h is the water depth, Ls is the wave length in shallow water, and Hs is the significant wave height. Values for the effective fetch were determined using typical fetches along the directions of frequent prevailing winds (north, north-east, and north-west) with respect to the location of the saltwater wedge. Results from the above calculations are summarized in Table 1.

Methodology

Field Sampling: A field sampling program was developed in order to obtain information on the plumes physical characteristics. The program has been in progress since the summer of 1998, and includes sampling along radial paths starting in the canal and proceeding into the lake. Initial sampling data only included surface and bottom readings. An extensive survey carried out in 1999 included data collection throughout the water column at intervals based on the intensity of stratification. This was achieved by collecting concentrated readings near the lake bed, where the saltwater wedge was evident. The data included readings for salinity, DO, and temperature at 12 stations near the IHNC and in the Lake Pontchartrain at the locations shown in Figure 1.

Physical Model: A physical model was also constructed to assess the spreading characteristics of the saltwater plume. The model has also been used to examine management scenarios for prevention of saltwater intrusion. Such scenarios include the introduction of a sill at the mouth of the canal at the entrance to the lake. Figure 2 shows an elevation snapshot of the plume as it enters the lake. There is a sill in place at an elevation of 1/3 of the lake depth.

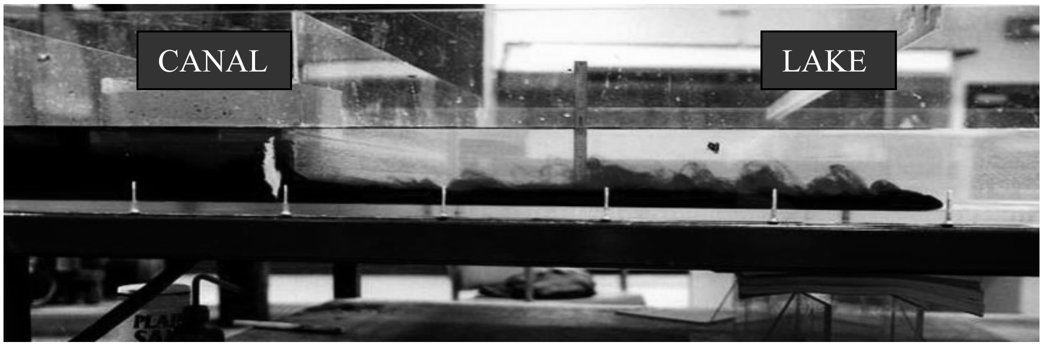

Figure 2 Profile view of the saltwater plume entering the lake; Δ_{sal}=6 ppt; ΔT=0°C; sill at 1/3 of lake depth

Results and Discussion

Systematic observations in the lake have shown frequent salinity, temperature, and DO stratification due to saltwater intrusion from the IHNC. The 1998 and 1999 field data showed higher density gradients during summer seasons, when there is little fresh water input in the lake due to drought conditions, low river flows, and increased evaporation. Figures 3 and 4 show typical vertical distribution of salinity and temperature through the water column of the lake. At times, the water temperatures in the salt wedge were found to be higher than the upper layer temperatures. With the specific heat of saltwater being higher than freshwater, the wedge sustained and carried these temperatures in the lake. Figure 3 illustrates the vertical temperature structure. Salinity profiles shown in Figure 4 are typical of the observed summer conditions and have very high maximum salinity gradients at about 4 m (average depth in the area

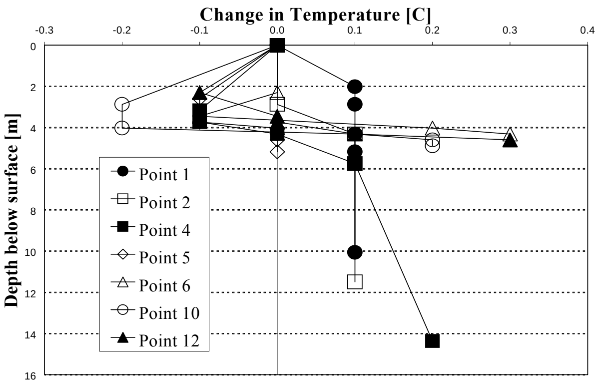

Figure 3 Selected temperature vertical profiles.
Wind speeds < 11ms^{-1}

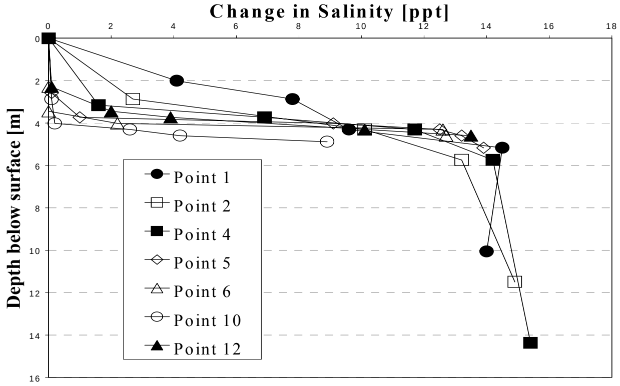

Figure 4 Selected salinity vertical profiles.
Wind speeds < 11ms^{-1}

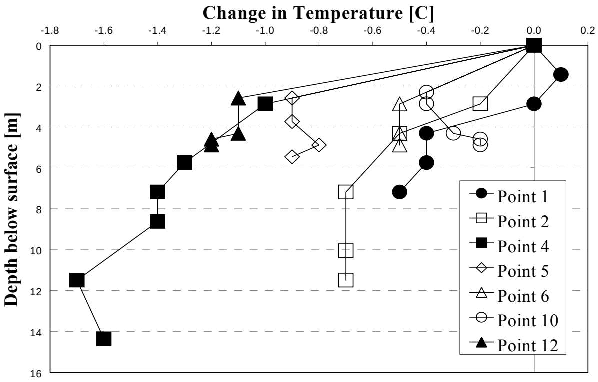

Figure 5 Selected temperature vertical profiles.
Wind speeds > 11ms^{-1}

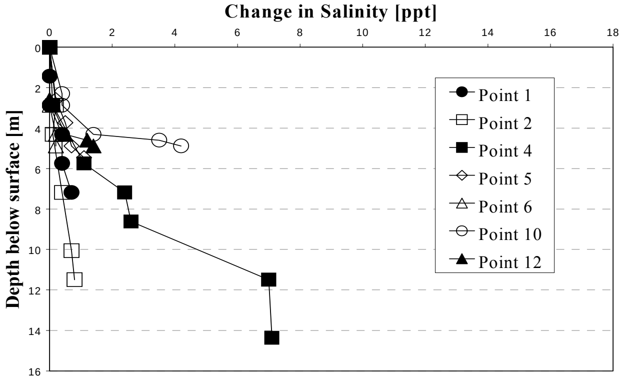

Figure 6 Selected salinity vertical profiles.
Wind speeds > 11ms^{-1}

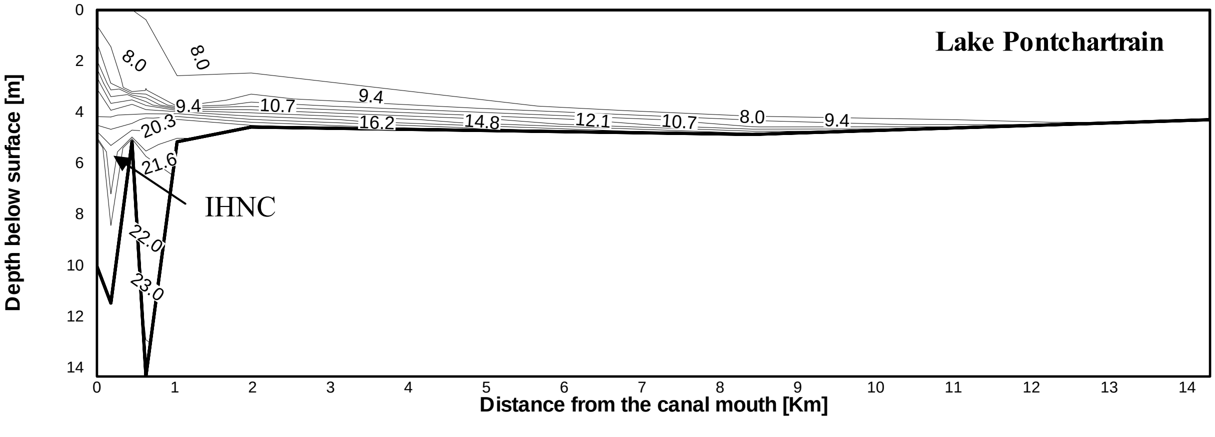

Figure 7 Typical plot of the summer observations of the arrested saline wedge. Salinity in ppt

is 4.6 – 5 m). Figures 5 – 6 show respectively the vertical profiles of temperature and salinity after a strong wind from the north; noticeable destratification of the salinity plume has occurred. The mixing process is assisted by bathymetry at the canal-lake junction (Figure 7). A scour hole and a dredge hole are present and extend radially at the mouth of the canal near the lake entrance. These holes provide a step-up in the bathymetry that serve as obstacles to the wedge propagation. Figure 7 also shows the profile view of the arrested saline wedge as it was measured on August 31, 1999. In determining values for the Richardson number, total velocity components were estimated. This included the use of a calibrated numerical model to estimate the current velocities (Haralampides, 2000), RMA2, and information from 3-D simulations using the POM model and field surveys performed by the United States Geological Survey (USGS) during 1996 in the area (Signell, 1995). The wave orbital velocities were estimated using Eqs. 2, 3, 4, and 5, and were added to the current velocities. The densities for both the upper and lower layer were calculated using local temperature and salinity values (Thomann and Mueller, 1987). For simplicity, the salt wedge was assumed to have zero velocity and a characteristic depth of 0.6 m, which is the average plume depth at half the intrusion length. Results for the Richardson number calculations are shown in Table 1, and in Figure 8.

Table 1 Summarized results for stability analysis. Values shown are averaged for wind direction and fetch

Wind Speed [ms^{-1}]	H_s [m]	T_s [m]	L_s [m]	u_{cur} [ms^{-1}]	u_s [ms^{-1}]	u [ms^{-1}]	Ri
5.36	0.17	1.58	3.90	0.03	0.00	0.03	43.88
10.73	0.50	2.57	10.20	0.06	0.15	0.21	1.09
14.31	0.76	3.15	14.62	0.09	0.35	0.44	0.25

A plume stability analysis was performed to determine what physical conditions are required to produce plume instability. A set of three wind speeds were selected representing mild, medium and gusty wind components for the area of study. Respectively, estimates of wave height, period, and wave length velocities were performed in order to get a relationship between wind speed and the Richardson number. Figure 8 clearly shows that wind velocities of approximately 11 ms^{-1} will in fact produce instability on the wedge interface and as a result mixing between the layers will occur. The same conditions also produce wave heights of nearly 0.5 m with a wave period of about 3 s. Field data from the fall of 1999 to the winter of 2000 confirmed that the plume was destabilized by winds from NW to NE between 10 - 12 ms^{-1}.

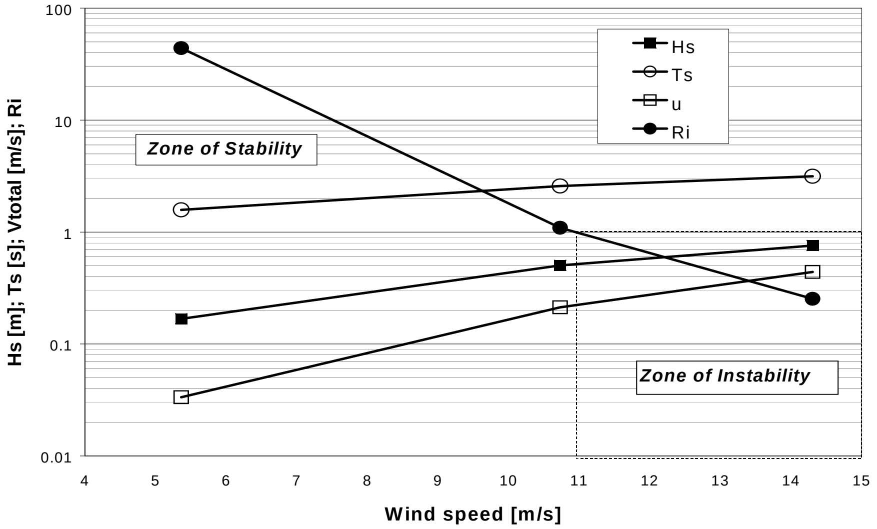

Figure 8 Plume stability analysis. Instability zone defined at: Ri<1; Ua>11 ms^{-1}.

Conclusions

This study illustrates the formation and expansion of a saltwater wedge from a navigation canal into a shallow lake, as well as the required conditions for plume instability. The stability analysis shows that wind shear induced by wind speeds of approximately 11 ms^{-1} can produce instabilities at the interface and eventually, at higher speeds, produce completely mixed fluid layers. Field data collected near the canal-lake junction show that the irregular bathymetry of the location increases the potential for instability and promotes mixing during inflow conditions. In addition, the stepwise increase in the depth from the canal to the lake serves as a sill and reduces the intrusion length. Laboratory experiment simulations performed using a sill at the canal mouth also reveal that such scenario produces local interface instability and higher entrainment of ambient water into the saltwater wedge. A combination of ongoing field surveys and laboratory experiments, and the future introduction of a three-dimensional numerical model will provide us with essential information on the plume dynamics. In addition, the numerical model will allow us to understand and study the effectiveness of proposed management scenarios for saltwater intrusion control.

References

Haralampides, K., 2000, *A Study of the Hydrodynamics and Salinity Regimes of the Lake Pontchartrain System*, Ph.D Dissertation, University of New Orleans, New Orleans, LA.

Kjerfve, Björn, 1988, *Hydrodynamics of Estuaries*, Volume I, Estuarine Physics, CRC Press, Florida.

Laenen, A., and Le Tourneau, A., P., 1996, *Upper Klamath Basin Nutrient-Loading Study – Estimate of Wind-Induced Resuspension of Bed Sediment During Periods of Low Lake Elevation*, U.S. Geological Survey, Report 95-414, Portland, Oregon.

Signell, Rich, 1995, *Three-Dimensional Circulation Modeling of Lake Pontchartrain*, Online Document, Obtained from www.crusty.er.usgs.gov on May, 9, 2000.

Thomann, V., R., and Mueller, J., A., John, 1987, *Principles of Surface Water Quality Modeling and Control*, Harper Collins Publishers Inc., New York, NY.

U.S. Army Corps of Engineers, 1984, *Shore Protection Manual*, Coastal Engineering Research Center, Department of the Army, Waterways Experiment Station, Vicksburg, Mississippi.

Yih, Chia-Shun, 1980, *Stratified Flows*, Academic Press, New York, NY.